Journal of Thermal Analysis, Vol. 54 (1998) 477-499

THE APPLICABILITY OF TMDSC TO POLYMERIC SYSTEMS
General theoretical description based on the full heat capacity formulation

*R. Scherrenberg**, *V. Mathot and P. Steeman*

DSM Research, P. O. Box 18, NL-6160MD Geleen, The Netherlands

Abstract

Temperature-modulated differential scanning calorimetry (TMDSC) has recently been introduced as a promising calorimetric technique. However, the added value of TMDSC in practice is still not very obvious, in particular with respect to crystallization and melting. An important reason is that the evaluation is less transparent than in case of other dynamic techniques since in TMDSC the response is also based on temperature. Moreover, the temperature program applied is very critical.

In this paper an overview is given of the different aspects of TMDSC using a general theoretical description based on the full heat capacity formulation. It is demonstrated that processes studied with the aid of TMDSC can simply be classified into three distinct regimes, depending on the time scale and the susceptibility of the process to the temperature modulation.

Keywords: base line heat capacity, crystallization, curing, deconvolution, DSC, excess heat capacity, glass-transition, linear response theory, melting, polymers, regime, TMDSC

Introduction

Differential scanning calorimetry (DSC) is a valuable technique that is frequently applied in the polymer field to study for instance melting and crystallization phenomena, glass-transition, thermal history and reaction kinetics (e.g. curing). Recently, temperature-modulated differential scanning calorimetry (TMDSC) has been introduced as an extension of DSC in which the usually linear or isothermal temperature program is superimposed with some type of temperature perturbation. The original idea was conceived and demonstrated by Reading and further developed by TA Instruments (MDSC) using a sinusoidal temperature modulation and a discrete Fourier transformation method for decon-

* Author to whom all correspondence should be addressed.

1418–2874/98/ $ 5.00

Akadémiai Kiadó, Budapest
Kluwer Academic Publishers, Dordrecht

volution [1–7]. In the mean-time, other DSC manufacturers such as Seiko (ODSC) [7], Perkin-Elmer (DDSC) [8] and Mettler (ADSC) [9] have also introduced TMDSC systems. These systems differ somewhat with respect to the experimental set-up as well as the data evaluation but in general the outcome of these different approaches is directly comparable.

At the introduction of TMDSC in 1993, it was claimed that this technique may become the preferred calorimetric technique for polymer characterisation [3]. The claimed practical benefits of TMDSC compared with conventional DSC include an improved sensitivity, a more efficient and accurate determination of the heat capacity as well as the separation of reversible second order processes (e.g. glass-transition) from irreversible processes such as recovery, recrystallization, evaporation and chemical reactions. It was also suggested that TMDSC gives better insight in the melting and crystallization phenomena of polymers.

Currently, a fast growing number of papers appears in the literature, describing in detail the TMDSC principle and related theory [10–16] as well as its applicability in a wide variety of processes such as absolute heat capacity [17–18], thermal conductivity [19–20], glass-transition [21–29], curing [30–33], miscibility [34–35], and crystallization and melting [36–40]. It has been demonstrated clearly that TMDSC has the ability to separate processes such as the glass-transition from enthalpy recovery, cold crystallization or the heat of reaction during curing. On the other hand, the claimed benefit of TMDSC with respect to the measurement of absolute heat capacity, thermal conductivity and especially melting and crystallization phenomena is not evident. Furthermore, the added value and applicablility of the so called full deconvolution method [10–12], based on the linear response theory, as compared with the simple deconvolution method, where the phase information is neglected, is still ambiguous. This situation is partly related to the fact that the application of the linear response theory to TMDSC proves to be more stringent and complex as compared with other dynamical techniques such as dynamical mechanical thermal analysis and dielectric spectroscopy. Due to this complexity, it is for a casual (TM)DSC user not obvious to recognize the added value as well as the numerous possible pitfalls connected with applying temperature modulation. In this paper, it will be attempted to give a clear overview using a general theoretical description, based on the so called full heat capacity concept [41]; i.e. splitting the heat capacity measured into a so called 'base-line' and 'excess' heat capacity. Accordingly, distinct regimes will be identified on the basis of the time scale and the susceptibility of the process to the temperature modulation. In a subsequent paper, the practical relevance of these regimes will be demonstrated on the basis of some characteristic TMDSC experiments.

General aspects of TMDSC

In TMDSC a modulated temperature profile is applied and the heat flow response is subsequently analysed using a Fourier transformation. This principle seems at first instance comparable with other dynamical techniques, such as dynamical mechanical thermal analysis (DMTA) and dielectric spectroscopy (DETA). However, the experimental conditions and data evaluation of TMDSC are even more critical than in case of DMTA and DETA because in TMDSC the temperature plays not only a role in the dynamic input but also with respect to the linear temperature variation $T_\beta(T_o+\beta_o t)$; Fig. 1) and the corresponding heat flow response $\Phi(T,t)$ (i.e. output). The latter is based on the temperature difference between the sample and reference cell. Moreover, the temperature modulation may affect the material properties to be measured. A mechanical equivalent of a TMDSC experiment woud be a DMTA measurement on top of a stress-strain test. In addition to the high complexity of TMDSC, a drawback is its limited dynamic range in comparison with DMTA and DETA. The modulation period can be varied roughly within 10 and 100 s corresponding to a frequency window of 10^{-2}–10^{-1} Hz.

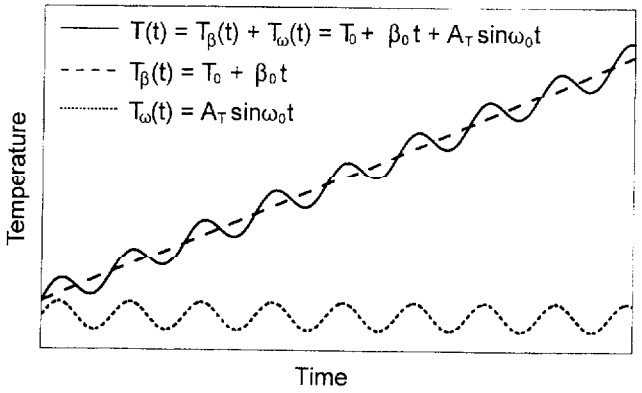

Fig. 1 An example of a time-temperature program in (TM)DSC. For illustrative reasons, the temperature program depicted does not comply with the important precondition that $\beta_o/(A_T\omega_o)<<1$

An important subject of discussion in the field of TMDSC is the relevance and applicability of the so called full deconvolution method which is based on the linear response theory [10–12]. Firstly, it is important to realise that the use of the linear response theory has only added value in case the time scale of the process studied is in the order of the time scale probed with (TM)DSC. For instance, processes that are significantly faster than the time scale of modulation will instantaneously respond to the temperature modulation and are therefore time-independent. On the other hand, processes that are appreciably slower than the

time scale of temperature modulation will not respond to the temperature modulation and consequently do not contribute to the heat flow response. For both cases, the use of the linear response theory has no added value. The linear response theory is only meaningful for a process with a time-dependence on the time scale of modulation provided that the following requirements are satisfied.

Invariance during a modulation period

The material properties (i.e. heat capacity) must be unaltered during a modulation period. For this reason, the choice of the temperature amplitude (A_T), especially in the case of an excess process, is critical.

Linearity of the process

The linear response theory implicitly assumes that linearity or the superposition principle holds; i.e. an input ax_1+bx_2 results in an output ay_1+by_2. If the heat flow response is non-linear, the determined properties will depend on the input. Linearity of the heat flow response is dependent on the process studied.

Apart from the requirements for the material response also instrumental aspects should be taken into account. The DSC system itself can contribute to non-linearity. In most cases, the currently available commercial DSC instruments are not able to apply the intended temperature variation directly to the whole sample. Limited heat conductivity, both in the DSC system and the sample introduce time delays which can be mistakenly regarded as the real heat flow response of the sample. For clarity, an ideal and linear heat flow response will be assumed in this paper. In practice, however, these effects cannot be disregarded. For more detailed information with respect to this subject the reader is referred to [13, 42].

Additional to the temperature modulation T_ω, an underlying linear temperature variation T_β ($T_o+\beta_o t$) can be applied (Fig. 1). In order to be able to compare the time scale of β_o directly with that of the temperature modulation, β_o can in principle be converted into a certain frequency, depending on the process studied. Although it is not straightforward to translate β_o into a frequency, especially in the case of phase transitions, Donth *et al.* [24, 43–45] have defined such a relationship for the glass-transition region. In view of the requirements for the linear response theory (i.e. invariance of the material properties), β_o has to be small (i.e. $\beta_o/(A_T\omega_o)<<1$). In that respect, quasi-isothermal conditions (i.e. $\beta_o=0$) can be considered as most favourable in TMDSC.

In this paper, the evaluation of the heat flow response is primarily based on the so called full heat-capacity based formulation (Appendix I) [41]. Such an approach simplifies the theoretical description of TMDSC considerably. On the basis of this description, a process studied with TMDSC can be classified into distinct regimes depending on its time scale and susceptibility of the process to the

temperature modulation. These different regimes will be defined in detail in the following paragraph, assuming that the linear response theory is applicable. For convenience, the description will be based on the sinusoidal temperature modulation. The description for other modulated temperature variations, such as a saw tooth and the iso-scan temperature program is principally analogous, but less transparent as compared with the sinusoidal modulation.

TMDSC Regimes

The base-line heat flow Φ_b (Regime I)

Regime I is representative for *the thermal behaviour of materials in absence of any excess heat flow response* (i.e. Φ_e=0). This regime includes the glass transition region without any net excess phenomena such as enthalpy recovery, crystallization and melting, curing or chemical reactions. The term 'net' is added because from a thermodynamic point of view the fractions of vitrified and unvitrified material do change in the glass transition region. However, these excess heat capacities are equal and of opposing sign. Consequently, these signals nullify each other [41].

The term 'net' is not relevant in the kinetic approach. The base-line heat capacity c_{p_b} of a polymeric material is largely determined by its molecular mobility, namely by torsional vibration and segmental motions. In the glassy state, relaxation processes are related to kinetically simple, quasi-independent motional events which can be described by an Arrhenius-type expression

$$\tau(T) \approx \tau_g e^{E_a/RT} \tag{1}$$

where τ(T) the relaxation time at a certain temperature, E_a the activation energy and τ_g the relaxation time at infinite temperature [46]. These motional events have relaxation times in the order of 10^{-13} s (i.e. $\tau_g \approx 10^{-13}$ s; $E_a << RT$) and are commonly denoted as non-cooperative motions, although several atoms participate in a motional event. The glass transition region, on the other hand, corresponds with motions of molecular segments. The relaxations times τ(T) corresponding to these so called cooperative motions are considerably larger as compared with the non-cooperative motions and can be, depending on the temperature, on the time scale of TMDSC (10–100 s) or even larger.

The time scales of the cooperative and non-cooperative motions are represented schematically in Fig. 2 by time distributions of the heat flow response. For illustrative purposes, these time distributions are represented by a Gaussian distribution. The time scales related to the temperature modulation (i.e. $2\pi/\omega_o$) and β_o are also illustrated in Fig. 2. The time scale corresponding to β_o has been positioned to the right of that of the temperature modulation considering $\beta_o/(A_T\omega_o) << 1$. The position of β_o on the time scale has been chosen somewhat arbitrary and can

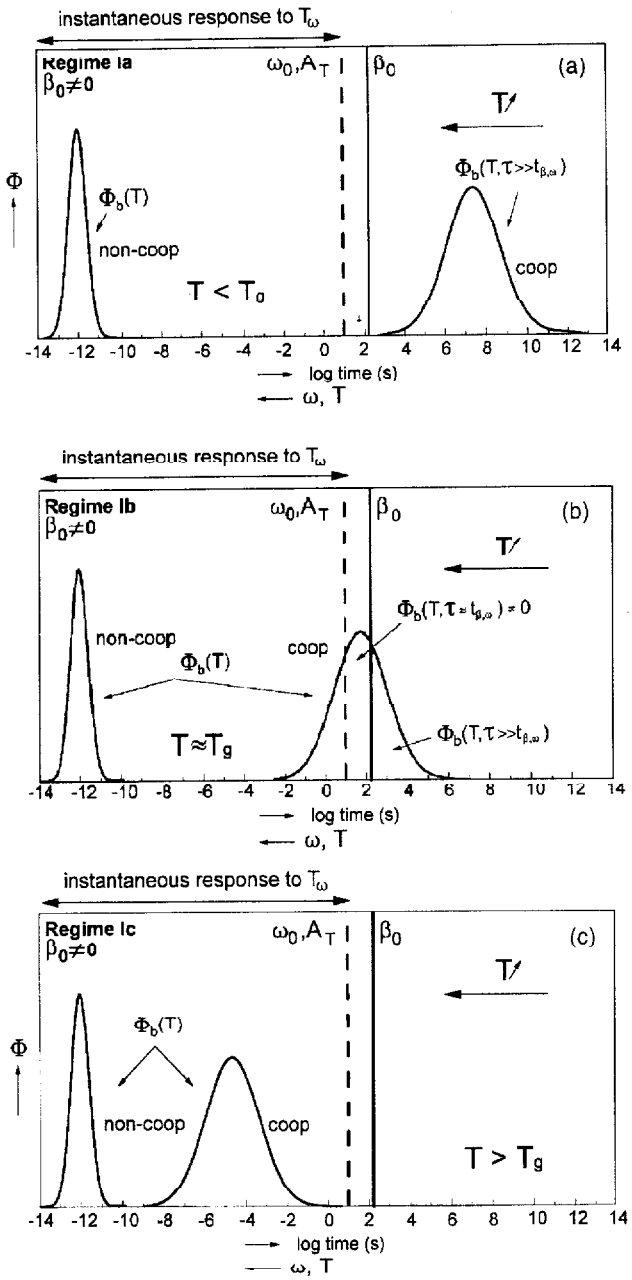

Fig. 2 Schematic representation of Regime I. Fig. (2a) and (2c) are representative for a material below and above the glass-transition region, respectively. Fig. (2b) is illustrative for the glass-transition region

shift to a certain extent with the temperature, depending on the activation energy of the process studied.

As illustrated in Fig. 2, the distribution corresponding to the non-cooperative motions is always situated completely left of the time scale probed with (TM)DSC (10–100 s) because the time scale of this type of motions is considerably shorter. The heat flow corresponding to these motions can therefore be regarded as time independent. On the other hand, the time scale of the cooperative motions can, due to the time–temperature interrelationship, be in the order of the time scales probed with (TM)DSC and hence can overlap at certain temperatures with the time scale of modulation. Accordingly, three subregimes can be identified (Fig. 2).

In Regime Ia (Fig. 2a), the time scale of the heat flow response Φ_b corresponding to the cooperative motions are located completely right of the modulation window, signifying that, in contrast to the non-cooperative motions, the cooperative motions are slow in comparison with the time scale of the experiment and will therefore not contribute to the heat flow response Φ_b. This regime is useful to describe the thermal properties of an amorphous polymer below the glass transition region.

In Regime Ic (Fig. 2c), the time scales of the heat flow response corresponding to both the cooperative and non-cooperative motions are situated completely left of the modulation window. Hence, the heat flow response will follow the applied temperature program instantaneously and can be regarded as time independent on the time scale of the modulation. Such a regime is representative for an amorphous polymer above the glass-transition region but also for a crystallizable polymer in the melt.

In the glass-transition region (Regime Ib), the time scale of the heat flow response Φ_b corresponding to the cooperative motions overlaps with the time scale of the temperature variation; i.e. the heat flow response comprises a time-dependent contribution (Fig. 2b). In case $\beta_o/(A_T\omega_o)<<1$, the total heat flow response $\Phi_b(T,t)$ can be separated into independent heat flow contributions, namely

$$\Phi_b(T,t) = \Phi_{b,\beta}(T,t) + \Phi_{b,\omega}(T,t) \tag{2}$$

where $\Phi_{b,\beta}(T,t)$ is the heat flow response a result of the underlying linear scanning rate β_o and is represented by (Eq. (I.5); Appendix I)

$$\Phi_{b,\beta}(T,t) = (c_{p_b}(T))_t\beta_o + \left(\sum_{i=1}^{i=n} w_i \frac{\partial h_i}{\partial t}\right)_I \tag{3}$$

The heat flow response $\Phi_{b,\omega}(T,t)$ is connected with the temperature modulation and can be expressed using the linear response theory provided that the re-

quirements described in paragraph 2, such as the material invariance during a modulation period, are satisfied (cf. Eq. (II.5): Appendix II).

$$\Phi_{b,\omega}(T,t) = \omega_o A_T \cos\omega_o t \left[c_{p_b}(T,t=0) + \int_0^t \dot{c}_{p_b}(T,t')\cos\omega_o t' dt' \right] + \\ + \omega_o A_T \sin\omega_o t \left[\int_0^t \dot{c}_{p_b}(T,t')\sin\omega_o t' dt' \right] \quad (4)$$

where $\dot{c}_{p_b}$ represents the variation of the base-line heat capacity with time (i.e. $\partial c_{p_b}/\partial t$). Analogous to other dynamical techniques, a so called magnitude of the complex heat capacity $[|c_p^*(T,\omega_o)|]$ as well as a real $[c_p'(T,\omega_o)]$ and an imaginary $[c_p''(T,\omega_o)]$ heat capacity can be defined (cf. Eq. (II.6), Appendix II).

$$c'_{p_b}(T,\omega_o) = c_{p_b}(T,t=0) + \int_0^\infty \dot{c}_{p_b}(T,t')\cos\omega_o t' dt' = |c^*_{p_b}(T,\omega_o)|\cos\delta(T,\omega_o) \quad (5)$$

$$c''_{p_b}(T,\omega_o) = \int_0^\infty \dot{c}_{p_b}(T,t')\sin\omega_o t' dt' = |c^*_{p_b}(T,\omega_o)|\sin\delta(T,\omega_o) \quad (6)$$

$$|c_p^*(T,\omega_o)| = \sqrt{(c'_{p_b}(T,\omega_o))^2 + (c''_{p_b}(T,\omega_o))^2} = \frac{A_{\Phi_\omega}(T,\omega_o)}{A_T\omega_o} \quad (7)$$

Equations (5)–(7) show that the real heat capacity comprises both an instantaneous and a time-dependent contribution while the imaginary heat capacity only involves a time-dependent contribution. The physical meaning of the imaginary heat capacity in Regime Ib is still subject to debate. The computation of an imaginary heat capacity raises the question where the corresponding amount of heat flow is observed in the DSC. Since heat capacity is not directly measured, but computed from the heat-flow and the temperature amplitudes (i.e. A_{Φ_ω} and A_T, respectively) only the heat flow response corresponding to the complex heat capacity is obtained from the experiment. The imaginary heat capacity is computed from the complex heat capacity and the phase lag δ (Appendix II) and is related to a fact that the enthalpy does not reach instantaneously its equilibrium value (i.e. $\partial h/\partial t \neq 0$). In contrast to DMTA, however, the imaginary component in TMDSC does not correspond with the real release of heat. At first instance, it was claimed that the imaginary heat capacity has no physical meaning and is caused by experimental artefacts [13]. Currently, it is believed that the imaginary heat capacity is related to some sort of entropy dissipative process [15, 47].

In contrast to Regime Ib, the heat flow response Φ_b is time-independent on the time-scale of modulation in Regime Ia and Ic. Hence, Eqs (3) and (4) can be simplified considerably into

$$\Phi_b(T,t) = \Phi_{b,\beta}(T,t) + \Phi_{b,\omega}(T,t) = c_{p_b}(T)\beta_o + c_{p_b}(T)\omega_o A_T \cos\omega_o t \tag{8}$$

Above equation nicely illustrates that in Regime Ia and Ic the second term $\Phi_{b,\omega}(T,t)$ is just proportional to the first derivative of the temperature modulation with a factor $c_{p_b}(T)$ and is therefore by definition $\pi/2$ phase shifted with respect to the temperature modulation. From Eq. (8) it can be simply derived that the amplitude of the heat flow corresponding to the temperature modulation (A_{Φ_ω}) is given by

$$A_{\Phi_\omega}(T) = \omega_o A_T c_{p_b}(T) \tag{9}$$

and

$$c_{p_b}(T) = \frac{A_{\Phi_\omega}(T)}{A_T \omega_o} \tag{10}$$

Notice that Eq. (10) is similar to Eq. (7) with the exception that the latter is frequency dependent. Equation (8) also reveals that in Regime Ia and Ic the heat capacity $c_{p_b}(T)$ is simply frequency independent and proportional to the ratio between the amplitude of the modulated heat flow A_{Φ_ω} and the temperature amplitude A_T. The determination of the heat capacity simply based on the ratio A_{Φ_ω} between A_T is better known as the simple deconvolution approach [1–7].

The heat flow in presence of excess phenomena (Regime II and III)

Additional to the heat flow response Φ_b connected with the base-line heat capacity, excess phenomena such as enthalpy recovery, crystallization and melting, and chemical reactions can contribute to the total heat flow response (Appendix I). The evaluation of the (TM)DSC heat flow response in presence of such excess phenomena is less straightforward in comparison with Regime I (e.g. material invariance) because the magnitude as well as the temperature dependence of the excess heat flow response Φ_e are generally considerably larger than Φ_b.

In case of an excess process, both the variation of the mass fraction with temperature ($\partial w_i/\partial T$) and time ($\partial w_i/\partial t$) are of importance (cf. Eq. (I.5); Appendix I). Firstly, the time scale (i.e. kinetics) of the excess process ($\partial w_i/\partial t$) has in all cases to be significantly longer than the time scale of modulation because otherwise the material properties vary during a modulation period and thus the requirement of material invariance is violated. For the same reason, the variation of the mass fraction w_i during a modulation as a result of the underlying scanning rate β_o has

to be negligible $\partial w_i/\partial T_\beta=0$, implying that quasi-isothermal conditions are preferable. Moreover, the susceptibility of the mass fraction w_i to the temperature modulation T_ω is of significance. In this respect, two different regimes, namely Regimes II and III, can be distinguished. *In Regime II, the existing mass fraction w_i is not influenced by the temperature modulation* (i.e. $\partial w_i/\partial T_\omega=0$). In other words, there is no contribution of the excess process to the heat flow response Φ_ω as a result of the temperature modulation (i.e. $c_{p_e}=0$). *In Regime III,* on the other hand, *the existing mass fraction w_i is varied by the temperature modulation* (i.e. $\partial w_i/\partial T_\omega\neq 0$).

Regime II ($\partial w_i/\partial T_\omega=0$)

The characteristics of Regime II are illustrated schematically in Fig. 3 for a curing process; i.e. a reducing mobility on increasing the degree of conversion w_i. Fig. 3a is representative for quasi-isothermal conditions ($\beta_o=0$) and Fig. 3b is valid in case of an underlying scanning rate β_o. For illustrative purposes, the time scale of the excess heat flow response is presented in Fig. 3 by a Gaussian type time distribution.

As illustrated in Fig. 3a, the time scale corresponding to the cooperative motions as well as the kinetics of the curing process ($\partial w_i/\partial t$) will shift under quasi-isothermal conditions with the degree of conversion w_i towards longer time-scales as a result of the reducing molecular mobility. At a certain point, the time scale of the cooperative motions can shift through the time scale of modulation (i.e. vitrification).

In case $\beta_o\neq 0$ (Fig. 3b), the situation is more complex because of the complex and counteracting influence of the temperature and the degree of conversion on the molecular mobility. Increasing the temperature increases the molecular mobility but also increases the conversion rate ($\partial w_i/\partial t$) of the curing process. The latter, on the other hand, will result in a lower molecular mobility. For these reasons, the time scale corresponding to Φ_b and Φ_e, as illustrated in Fig. 3b, is quite arbitrary and is very dependent on the temperature and process studied.

Analogous to Regime I, the total heat flow response can be considered as two independent heat flow contributions (i.e. $\beta_o/(A_T\omega_o)<<1$).

$$\Phi(T,t)=\Phi_\beta(T,t)+\Phi_\omega(T,t) \tag{11}$$

with (cf. Eq. (I.5); Appendix I.5)

$$\Phi_\beta(T,t)=\left(c_{p_b}(T)+c_{p_e}(T)\right)\beta_o+\left(\sum_{i=1}^{i=n}w_i\frac{\partial h_i}{\partial t}+\sum_{i=1}^{i=n}h_i\frac{\partial w_i}{\partial t}\right)_T \tag{12}$$

In Regime II, the excess process is not susceptible to the temperature modulation (i.e. $\partial w_i/\partial T_\omega = 0$) and hence *the heat flow response* $\Phi_\omega(T,t)$ *is uniquely determined by the base-line heat capacity* c_{p_b}. This implies that in Regime II the expression for $\Phi_\omega(T,t)$ is simply identical to Eq. (4). This is a very important feature that enables the separation between the base-line heat capacity and an excess heat flow contribution such as for instance enthalpy recovery, cold crystallization or a heat of reaction superimposed on a vitrification process. As already mentioned, the above is only valid under the condition of linearity and invariance of the material properties, implying that $\partial w_i/\partial T_\beta$ and $\partial w_i/\partial t$ during a modulation period have to be negligible. Additionally, the kinetics $\partial w_i/\partial t$ may not be influenced significantly by the temperature modulation T_ω. Consequently, the choice

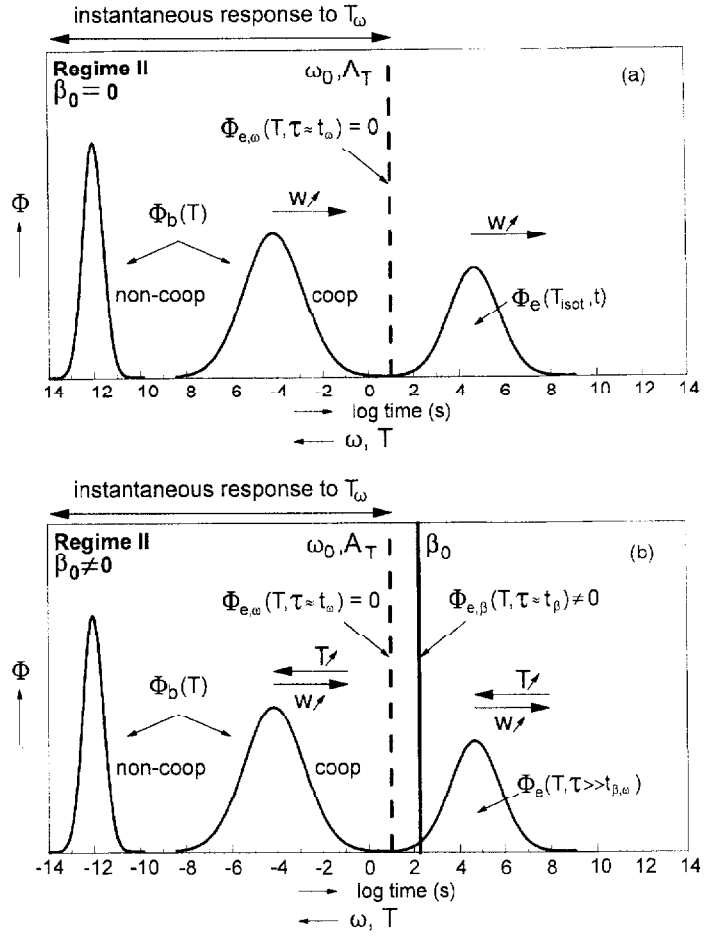

Fig. 3 Schematic representation of Regime II. Fig. (3a) and (3b) are illustrative for a curing process under quasi-isothermal (β_0=0) conditions and with a underlying linear temperature variation $T_\beta(\beta_0 \neq 0)$, respectively

of the linear temperature variation β_o, the isothermal temperature and the temperature amplitude A_T are very critical. In this respect, quasi-isothermal conditions are recommendable.

In case of an instantaneous heat flow response of the base-line heat capacity c_{p_b} to the temperature modulation, the total heat flow is represented by

$$\Phi(T,t) = \left(c_{p_b}(T) + c_{p_e}(T)\right)\beta_o + \left(\sum_{i=1}^{i=n} h_i \frac{\partial w_i}{\partial t}\right)_T + c_{p_b}(T)\omega_o A_T \cos\omega_o t \qquad (13)$$

The heat flow response connected with variation of the mass fraction w_i with time (i.e. $\partial w_i/\partial t$) has been included in the above equation because, as a result of $\beta_o/(A_T\omega_o)\ll 1$, β_o can be in the order that the time-dependence cannot longer be neglected (cf. Appendix I). Under quasi-isothermal conditions, the heat flow response $\Phi(T,t)$ can be further simplified into

$$\Phi(T,t) = \Phi_{isot}(T_o,t) + \Phi_\omega(T,t) = \left(\sum_{i=1}^{i=n} h_i \frac{\partial w_i}{\partial t}\right)_{T_o} + c_{p_b}(T)\omega_o A_T \cos\omega_o t \qquad (14)$$

Similar to Regime Ia and Ic, the base-line heat capacity can be derived from the ratio between the amplitude of $\Phi_\omega(T,t)$ and the temperature amplitude A_T (cf. Eq. (10)).

Regime III ($\partial w_i/\partial T_\omega \neq 0$)

The characteristics of Regime III are illustrated schematically in Fig. 4a and b by two examples: $\beta_o=0$ and $\beta\neq 0$, respectively. The preconditions in Regime III are analogous to Regime II (i.e. $\partial w_i/\partial T_\beta=0$ or $\partial w_i/\partial t=0$) with the important complication that there is an additional heat flow response $\Phi_{e,\omega}$ as a result of the susceptibility of the existing mass fraction w_i to the temperature modulation T_ω (i.e. $\partial w_i/\partial T_\omega\neq 0$). In the literature, this phenomenon is commonly referred to as the temperature reversibility of a process and is represented in Fig. 4 by an additional time distribution.

Figure 4a represents a quasi-isothermal measurement with a certain susceptibility of the excess process to the temperature modulation and with a decrease of the mobility as a function of the time. In that respect, Fig. 4a is typical for an isothermal crystallization process with so called reversible melting and crystallization phenomena. Figure 4b, on the other hand, is representative for a process with a temperature susceptible fraction. The increase of the mobility is primarily related with the decrease of the mass fraction w_i with the temperature. Such a situation is characteristics for the melting process where the crystalline mass fraction decreases with the temperature.

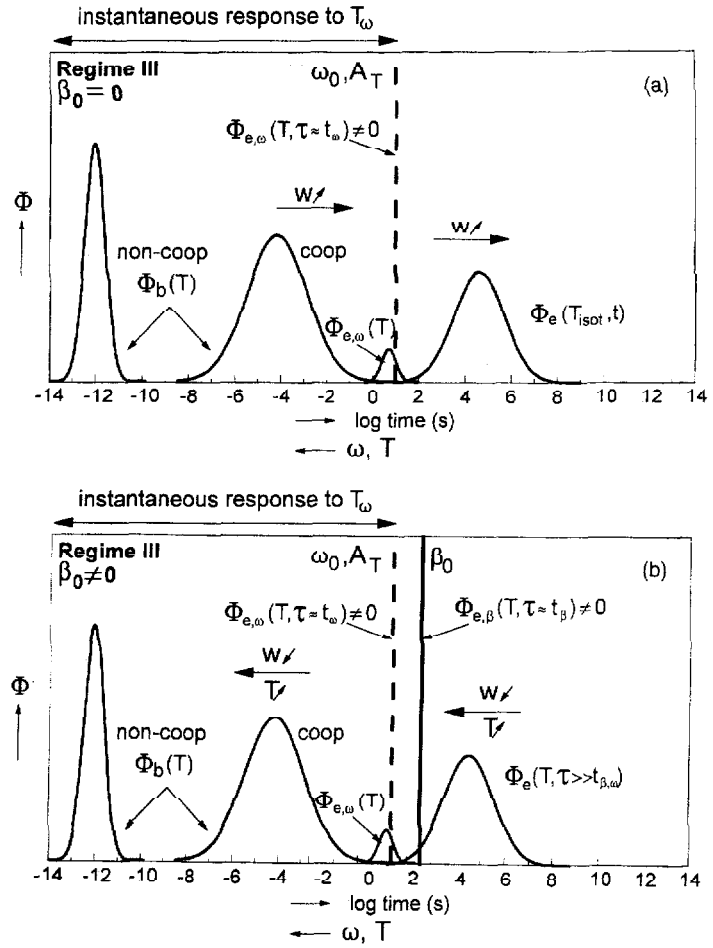

Fig. 4 Schematic representation of Regime III. Fig. (4a) is representative for a quasi-isothermal crystallization process (β_0=0). Figure (4b) is illustrative for a melting process with an underlying linear temperature variation $T_\beta(\beta_0 \neq 0)$

Analogous to Regime II, one could derive an expression for the heat flow response on the basis of the linear response theory. In contrast to Regime II, however, *the heat flow response* Φ_ω *is not uniquely determined by the base-line heat capacity* (i.e. $\partial w_i / \partial T_\omega \neq 0$). Consequently, the separation of the base-line and excess heat capacity is not feasible in Regime III. Similar to Regime II, quasi-isothermal conditions are preferable with the preconditions that at the isothermal temperature $\partial w_i / \partial t$ is negligible on the time scale of the temperature modulation and $\partial w_i / \partial t$ is not influenced significantly by the temperature amplitude A_T applied. In contrast to Regime II, however, the relevance of the linear response theory under quasi-isothermal conditions is somewhat disputable because, apart

from the question of linearity of the melting and crystallization process, the requirement of material invariance is intrinsically violated in Regime III due to fact that $\partial w_i/\partial T_\omega \neq 0$. In most cases this leads to complete failure of the TMDSC method. Only in the case of a very small susceptibility of the excess process to the temperature modulation (i.e. $\partial w_i/\partial T_\omega \approx 0$) it is reasonable to apply the linear response theory.

In Regime III, the total heat flow response $\Phi(T,t)$ is composed of two independent heat flow contributions $\Phi_\beta(T,t)$ and $\Phi_\omega(T,t)$. The heat flow response response $\Phi_\beta(T,t)$ to the linear scanning rate is identical to that in Regime II (i.e. Eq. (12)). On the other hand, the heat flow response $\Phi_\omega(T,t)$ connected with the temperature modulation is represented by

$$\Phi_\omega(T,t) = \omega_o A_T \cos\omega_o t \left[c_{p_b}(T,t-0) + c_{p_e}(T,t=0) + \int_0^t \left(\dot{c}_{p_b}(T,t') + \dot{c}_{p_e}(T,t') \right) \cos\omega_o t' \, dt' \right] + \omega_o A_T \sin\omega_o t \left[\int_0^t \left(\dot{c}_{p_b}(T,t') + \dot{c}_{p_e}(T,t') \right) \sin\omega_o t' \, dt' \right] \quad (15)$$

It is important to emphasize again that, in contrast to Regime II, the heat flow response $\Phi_\omega(T,t)$ now comprises an excess heat flow response originating from the fraction of material that is susceptible to the temperature modulation. This implies that the ability to separate the base-line heat capacity from an excess heat flow contribution is no longer valid in Regime III. Under the preferred quasi-isothermal conditions and assuming an instantaneous heat flow response to the applied temperature modulation, the expression for the total heat flow response $\Phi(T,t)$ can be simplified considerably into

$$\Phi(T,t) = \Phi_{isot}(T_o,t) + \Phi_\omega(T,t) = \left(\sum_{i=1}^{i=n} h_i \frac{\partial w_i}{\partial t} \right)_{T_o} + \left[c_{p_b}(T) + c_{p_e}(T) \right] \omega_o A_T \cos\omega_o t \quad (16)$$

Conclusions

The general theoretical description outlined in this paper demonstrates that, based on the full heat capacity formulation, processes studied with TMDSC can simply be classified into three distinct Regimes depending on the time scale and the susceptibility of the existing mass fraction to the temperature modulation (i.e. $\partial w_i/\partial T_\omega$). The characteristics of these Regimes have been summarized in Table 1, assuming linearity and material invariance during the modulation period.

Typical practical examples where the use of the full deconvolution method is relevant have also been included in Table 1.

The intrinsic higher sensitivity and the ability to separate the base-line heat capacity c_{p_b} from an excess heat flow (Regime II) is undoubtedly important added value of TMDSC as compared with conventional DSC, in particular with respect to the glass transition region. Nonetheless, this added value has to be put into the right perspective because of its restricted dynamic range as compared with DMTA and DETA. Additionally, one has to realise that the added value is restricted to those cases which involve excess processes that are not susceptible to the temperature modulation (i.e. $\partial w_i/\partial T_\omega=0$). Otherwise, the excess process contributes to the modulated heat flow response Φ_ω and thus is no longer uniquely determined by the base-line heat capacity c_{p_b} (Regime III). Therefore, the elucidation of the glass transition during melting in for instance a polymer blend is not feasible with TMDSC.

The requirement of linearity and material invariance on the time scale of modulation is also an essential precondition in TMDSC that, especially in the case of excess phenomena such as crystallization and melting, limits its applicability substantially. The required linear response with temperature and the strong temperature dependence of the kinetics in combination with the generally large heat flow, imply that the temperature program applied is very critical (Regime II and III). For that reason, the linear underlying scanning rate β_o has to be small (i.e. $\beta_o/(A_T\omega_o)<<1$) and preferably $\beta_o=0$ during the period of temperature modulation (i.e. quasi-isothermal conditions). In that respect, so called step-wise quasi-isothermal measurements are beneficial. In view of the material invariance, the choice of the isothermal temperature during a quasi-isothermal experiment is also crucial because the variation of the mass fraction w_i with time (i.e. $\partial w_i/\partial t$) has to be insignificant on the time scale of the temperature modulation. Finally, the temperature amplitude A_T applied has to be chosen small enough not to influence the kinetics of the excess process studied. Despite these very strict conditions, TMDSC has added value, including crystallization and melting, as will be outlined in more detail in a subsequent paper.

Summarizing the expectation that TMDSC would become a preferred calorimetric technique in polymer characterization has to be qualified. It is more realistic to regard TMDSC as a valuable extension of DSC which is primarily advantageous in case of overlapping processes involving excess processes that are not susceptible to the temperature modulation such as curing (Regime II).

Table 1 Characteristics of the different TMDSC regimes assuming that the contribution of $\partial w_i/\partial t$ and $\partial w_i/\partial T_\beta$ to the modulated heat flow response Φ_ω is negligible on the time scale modulation. Typical practical examples have been included and are denotec by an asterisk (*)

	Deconvolution method	Conditions	Characteristics
Regime I	full	$\Phi_e(T,t)=0$	– no excess phenomena
		$\Phi_\omega(T,t)=\Phi_{b,\omega}(T,t)$	– time-dependent heat flow response on time scale of temperature modulation
		$\tau\approx t_\omega$	
		$\delta\neq 0$	*base-line heat capacity c_{p_b} in the glass-transition region in absence of excess phenomena (e.g. enthalpy recovery, heat of reaction)
	simple	$\Phi_e(T,t)=0$	– no excess phenomena
		$\Phi_\omega(T)=\Phi_{b,\omega}(T)$	– time-independent heat flow response on time scale of temperature modulation; instantaneous heat flow response
		$\tau<<t_\omega;\ \tau>>t_\omega$	
		$\delta=0$	
			*base-line heat capacity c_{p_b} outside glass-transition and melting/crystallization region
Regime II	full	$\Phi_e(T,t)\neq 0$	– excess phenomena
		$\partial w_i/\partial T_\omega=0$	– time-dependent heat flow response on time scale of temperature modulation
		$\Phi_{e,\omega}(T,t)=0$	– excess heat flow response **not susceptible** to temperature modulation
		$\Phi_\omega(T,t)=\Phi_{b,\omega}(T,t)$	– heat flow response corresponding to the temperature modulation **uniquely** determined by base-line heat capacity c_{p_b}
		$\tau\approx\tau_\omega$	
		$\delta\neq 0$	
			*separation of the glass-transition region from excess phenomena (e.g. enthalpy recovery, heat of reaction, cold crystallization and evaporation)

Table 1 Continued

	Deconvolution method	Conditions	Characteristics
Regime II	simple	$\Phi_e(T,t)\neq 0$	– excess phenomena
		$\partial w_i/\partial T_\omega=0$	– time-irdependent heat flow response on time scale of temperature modulation;
		$\Phi_{e,\omega}(T,t)=0$	instantaneous heat flow response
		$\Phi_\omega(T)=\Phi_{b,\omega}(T)$	– excess heat flow response **not susceptible** to temperature modulation
		$\tau<<t_\omega$; $\tau>>t_\omega$	– heat flow response corresponding to the temperature modulation
		$\delta=0$	**uniquely** determined by base-line heat capacity c_{p_b}
			*separation of the base-line heat capacity from excess phenomena (e.g. evaporation, heat of reaction) outside the glass-transition or melting/crystallization region
Regime III	full	$\Phi_e(T,t)\neq 0$	– excess phenomena
		$\partial w_i/\partial T_\omega\neq 0$	– time-dependent heat flow response on time scale of temperature modulation
		$\Phi_{e,\omega}(T,t)\neq 0$	– excess heat flow response susceptible to temperature modulation
		$\Phi_\omega(T,t)=[\Phi_{b,\omega}(T,t)$	– heat flow response comprises both a base-line and excess heat capacity contribution
		$+\Phi_{e,\omega}(T,t)]$	*melting and crystallization phenomena on time scale of the temperature modulation
		$\tau\approx t_\omega$; $\delta\neq 0$	
	simple	$\Phi_e(T,t)\neq 0$	– excess phenomena
		$\partial w_i/\partial T_\omega\neq 0$	– time-independent heat flow response on time scale of temperature modulation;
		$\Phi_{e,\omega}(T,t\approx t_\omega)\neq 0$	*instantaneous heat flow response*
		$\Phi_\omega(T)=[\Phi_{b,\omega}(T)$	– excess heat flow response **susceptible** to temperature modulation
		$+\Phi_{e,\omega}(T)]$	– heat flow response comprises **both** a base-line and excess heat capacity contribution
		$\tau<<t_\omega$; $\tau>>t_\omega$	*melting and crystallization phenomena outside the time scale of

Appendix I

The heat flow response in conventional DSC

The enthalpy variation $dh(T,t)$ is both a function of temperature T and time t. Separation into two independent contributions gives

$$dh(T,t) = \left(\frac{\partial h}{\partial T}\right)_t dT + \left(\frac{\partial h}{\partial t}\right)_T dt \tag{I.1}$$

Subsequently, the total heat flow response $\Phi(T,t)$ can be described as

$$\Phi(T,t) = \frac{dh(T,t)}{dt} = \left(\frac{\partial h}{\partial T}\right)_t \frac{dT}{dt} + \left(\frac{\partial h}{\partial t}\right)_T \tag{I.2}$$

The first term of Eq. (I.2) represents the instantaneous response of the heat flow and can be written as

$$\Phi(T) = \left(\frac{\partial h}{\partial T}\right)_t \frac{dT}{dt} = \left(\sum_{i=1}^{i=n} w_i \frac{\partial h_i}{\partial T} + \sum_{i=1}^{i=n} h_i \frac{\partial w_i}{\partial T}\right)_t \frac{dT}{dt} = \left(c_{p_b}(T) + c_{p_e}(T)\right)_t \frac{dT}{dt} \tag{I.3}$$

where $c_{p_b}(T)$ and $c_{p_e}(T)$ are the time independent base-line and excess heat capacity [41] respectively and h_i and w_i the enthalpy and mass fraction of phase i. The time-dependent contribution in (I.2) is given by

$$\left(\frac{\partial h}{\partial t}\right)_T = \left(\sum_{i=1}^{i=n} w_i \frac{\partial h_i}{\partial t}\right)_T + \left(\sum_{i=1}^{i=n} h_i \frac{\partial w_i}{\partial t}\right)_T \tag{I.4}$$

The first term of Eq. (I.4) symbolizes the time-dependence of the enthalpy and the second term the time-dependence (i.e. kinetics) of the excess process. For clarity, the total heat flow response for a conventional DSC experiment with an underlying linear scanning rate β_o can be represented by two independent heat flow contributions, the base-line heat flow $\Phi_{b,\beta}$ and the exess heat flow $\Phi_{e,\beta}$, respectively

$$\Phi_{b,\beta}(T,t) = \left(\sum_{i=1}^{i=n} w_i \frac{\partial h_i}{\partial T}\right)_t \beta_o + \left(\sum_{i=1}^{i=n} w_i \frac{\partial h_i}{\partial t}\right)_T = (c_{p_b}(T))_t \beta_o + \left(\sum_{i=1}^{i=n} w_i \frac{\partial h_i}{\partial t}\right)_T \tag{I.5}$$

$$\Phi_{e,\beta}(T,t) = \left(\sum_{i=1}^{i=n} h_i \frac{\partial w_i}{\partial T}\right)_t \beta_o + \left(\sum_{i=1}^{i=n} h_i \frac{\partial w_i}{\partial t}\right)_T - (c_{p_e}(T))_t \beta_o + \left(\sum_{i=1}^{i=n} h_i \frac{\partial w_i}{\partial t}\right)_T \quad (I.5)$$

In conventional DSC, the linear temperature variation with time (i.e. β_o) is generally so large that the time-dependent heat flow contributions in Eq. (I.5) can be neglected. For that reason, these time-dependent terms are commonly disregarded in textbooks on DSC. Nonetheless, the time-dependent heat flow contributions become more significant, especially in case of an excess process, on lowering the scanning rate and uniquely determines the heat flow response under isothermal conditions.

Appendix II

Linear response in TMDSC

This appendix describes the heat flow response as a consequence of a temperature modulation T_ω. In that respect, so called quasi-isothermal conditions (i.e. β_o=0) are considered in which a cyclic temperature variation is applied around an isothermal temperature T_o.

If an intensive system variable such as the temperature is changed, the extensive parameter, e.g. the enthalpy $h(T,t)$, is described by the auto-correlation function or so called retardation function. In TMDSC the retardation function is represented by the time-dependent heat capacity $c_p(T,t)$. Assuming linearity and material invariance, the enthalpy variation can be expressed by a convolution.

$$h(T,t) - h(T,t=0) = \int_0^t c_p(T,t-t')\dot{T}(t')dt' \quad (II.1)$$

The linearity is expressed by the additive properties of the integral in Eq. (II.1). The causality can be seen from the integration limits; t' covers the whole history after arriving at the measurement temperature up to the actual time t. The lower limit of the integral has been set to zero because contributions from t<0 are assumed to be negligible. The 'memory' function $c_p(T,t-t')$ evaluates the temperature history given by the scan rate $\dot{T}(t')=\beta(t')$. In a TMDSC measurement, the heat flow response $\Phi(T,t)$, using Eq. (I.2), is given by

$$\Phi(T,t) = \left(\frac{\partial h}{\partial T}\right)_t \beta(t) + \left(\frac{\partial h}{\partial t}\right)_T =$$

$$= c_p(T,t=0)\beta(t) + \int_0^t \dot{c}_p(T,t-t')\beta(t')dt' + \left[\int_0^t \frac{\partial c_p(T,t-t')}{\partial T}\beta(t')dt'\right]\beta(t) \quad (II.2)$$

where $\dot{c}_p = \partial c_p/\partial t$. In view of the required material invariance, the variation of the heat capacity with the temperature (i.e. $\partial c_p/\partial T$) has to be negligible and therefore, combined with changing t' and $t-t'$, Eq. (II.2) can be simplified into

$$\Phi(T,t) = c_p(T,t=0)\beta(t) + \int_0^t \dot{c}_p(T-t')\beta(t-t')dt' \qquad \text{(II.3)}$$

The first term of Eq. (II.3) represents the instantaneous response to the cyclic temperature variation and the second term is a convolution describing the time-dependent contribution of the heat flow as a result of the cyclic temperature variation around T_o. The linearity is expressed by the additive properties of this convolution. The causality can be seen from the integration limits; t' covers the whole history after arriving at the measurement temperature up to the actual time t. The lower limit of the integral has been set to zero because contributions from $t<0$ are assumed to be negligible. Under quasi-isothermal conditions, the temperature variation $\beta(t-t')$ is given by

$$\beta(t-t') = \omega_o A_T \cos\omega_o(t-t') = \omega_o A_T(\cos\omega_o t\cos\omega_o t' + \sin\omega_o t\sin\omega_o t') \qquad \text{(II.4)}$$

Substitution of Eq. (II.4) in (II.3) yields

$$\Phi_\omega(T,t) = \omega_o A_T \cos\omega_o t\left[c_p(T,t=0) + \int_0^t \dot{c}_p(T,t')\cos\omega_o t'dt'\right] + \omega_o A_T \sin\omega_o t\left[\int_0^t \dot{c}_p(T,t')\sin\omega_o t'dt'\right] \qquad \text{(II.5)}$$

For $t\to\infty$ $\dot{c}_{p_b}(T,t')$ goes to zero and consequently, the in-phase and out-of-phase heat capacity, $c_p'(T,\omega_o)$ and $c_p''(T,\omega_o)$, can be defined

$$c_p'(T,\omega_o) \equiv c_p(T,t=0) + \int_0^\infty \dot{c}_p(T,t')\cos\omega_o t'dt' \qquad \text{(II.6)}$$

$$c_p''(T,\omega_o) \equiv \int_0^\infty \dot{c}_p(T,t')\sin\omega_o t'dt' \qquad \text{(II.7)}$$

Notice that in contrast to $c_p''(T,\omega_o)$, $c_p'(T,\omega_o)$ comprises the instantaneous response of the heat capacity $c_p(T,t=0)$. Inserting Eqs (II.6) and (II.7) into Eq. (II.5) gives

$$\Phi_\omega(T,t) = c_p'(T,\omega_o)\omega_o A_T\cos\omega_o t + c_p''(T,\omega_o)\omega_o A_T\sin\omega_o t \qquad \text{(II.8)}$$

Equation (II.8) can also be represented by

$$\Phi_\omega(T,t) = |c_p^*(T,\omega_o)|\omega_o T_a \cos(\omega_o t - \delta(T,\omega_o)) \quad \text{(II.9)}$$

where $|c_p^*(T,\omega_o)|$ and $\delta(T,\omega_o)$ are the magnitude of the complex heat capacity and the phase angle, respectively.

On the basis of Eq. (II.9), the following relations can be derived

$$c_p'(T,\omega_o) = |c_p^*(T,\omega_o)|\cos\delta(T,\omega_o) \quad \text{(II.10a)}$$

$$c_p''(T,\omega_o) = |c_p^*(T,\omega_o)|\sin\delta(T,\omega_o) \quad \text{(II.10b)}$$

$$|c_p^*(T,\omega_o)| = \sqrt{(c_p'(T,\omega_o))^2 + (c_p''(T,\omega_o))^2} = \frac{A_{\Phi_\omega}(T,\omega_o)}{A_T\omega_o} \quad \text{(II.10c)}$$

$$\tan\delta(T,\omega_o) = \frac{c_p''(T,\omega_o)}{c_p'(T,\omega_o)} \quad \text{(II.10d)}$$

where $A_{\Phi_\omega}(T,\omega_o)$ is the amplitude of the heat flow response corresponding to the temperature modulation.

Synopsis

t	time
t_ω	characteristic time scale of temperature modulation
t_β	characteristic time scale of linear underlying scanning rate
τ	characteristic time scale of process
T	temperature
T_o	initial temperature, isothermal temperature
β	scanning rate, $\beta = dT/dt$
β_o	linear scanning rate
A_T	temperature amplitude
T_ω	modulated temperature variation ($A_T\sin\omega_o t$)
T_β	linear temperature variation ($T_o+\beta_o t$)
p	period
ω_o	$=2\pi/p$
c_p	heat capacity
c_{p_b}	base-line heat capacity
c_{p_e}	excess heat capacity
w_i	mass fraction of phase i
h_i	enthalpy of phase i
$\partial w_i/\partial T_\omega$	variation of the mass fraction w_i due to the modulated temperature variation T_ω

$\partial w_i/\partial T_\beta$ variation of the mass fraction w_i due to the conventional temperature variation T_β
$\partial w_i/\partial t$ variation of the mass fraction w_i with time
Φ total heat flow response
Φ_β conventional heat flow response with linear scanning rate β_o
Φ_ω modulated heat flow response
Φ_{isot} conventional heat flow response at the isothermal temperature T_o
Φ_b base-line heat flow response connected with base-line heat capacity
Φ_e excess heat flow response connected with excess heat capacity
$\Phi_{b,\beta}$ conventional base-line heat flow response
$\Phi_{e,\beta}$ conventional excess heat flow response
$\Phi_{b,\omega}$ modulated base-line heat flow response
$\Phi_{e,\omega}$ modulated excess heat flow response
A_{Φ_ω} amplitude of heat flow response connected with Φ_ω
$\dot{c}_p$ $= \partial c_p/\partial t$
c_p' real heat capacity
c_p'' imaginary heat capacity
$|c_p^*|$ magnitude of the complex capacity
δ phase angle

References

1 M. Reading, Trends Polym. Sci., 1 (1993) 248.
2 M. Reading, Thermochim. Acta, 238 (1994) 295.
3 S. R. Sauerbrunn, B. S. Crowe and M. Reading, Polym. Mater. Sci. Eng., 68 (1993) 269.
4 M. Reading, D. Elliot and V. L. Hill, J. Thermal Anal., 40 (1993) 949.
5 M. Reading, A. Luget and R. Wilson, Thermochim. Acta, 238 (1994) 295.
6 P. S. Gill, S. R. Sauerbrunn and M. Reading, J. Thermal Anal., 40 (1993) 931.
7 W. J. Sinchina and N. Nakamura, ODSC software, Seiko Instr. Product Detail 5.
8 M. P. DiVito, R. B. Cassel, M. Margulies and S. Goodkowsky, Am. Lab., 27 (1995) 28.
9 R. Riesen, G. Widmann and R. Truttmann, Thermochim. Acta, 268 (1995) 1.
10 J. E. K. Schawe, Thermochim. Acta, 260 (1995) 1.
11 J. E. K. Schawe and G. W. H. Höhne, Thermochim. Acta, 287 (1996) 213.
12 J. E. K. Schawe, Thermochim. Acta, 271 (1996) 127.
13 B. Wunderlich, A. Boller, I. Okazaki and S. Kreitmeier, Thermochim. Acta, 282/283 (1996) 143.
14 B. Wunderlich, Y. Jin and A. Boller, Thermochim. Acta, 238 (1994) 277.
15 J. E. K. Schawe and G. W. H. Höhne, Thermochim. Acta, 287 (1996) 213.
16 B. Wunderlich, J. Thermal Anal., 48 (1997) 207.
17 A. Boller, Y. Jin and B. Wunderlich, J. Thermal Anal., 42 (1994) 307.
18 T. Ozawa and K. Kanari, Thermochim. Acta, 288 (1996) 39.
19 S. M. Marcus and R. L. Blaine, Thermochim. Acta, 243 (1994) 231.
20 S. R. Aubuchon and R. L. Blaine, Therm. Conduct., 23 (1996) 66.
21 M. Song, A. Hammiche, H. M. Pollock, D. J. Hourston and M. Reading, Polymer, 36 (1995) 3313.
22 A. Boller, C. Schick and B. Wunderlich, Thermochim. Acta, 266 (1995) 97.
23 J. M. Hutchinson and S. Montserrat, J. Thermal Anal., 47 (1996) 103.

24 A. Hensel, J. Dobbertin, J. E. K. Schawe, A. Boller and C. Schick, J. Thermal Anal., 46 (1996) 935.
25 J. M. Hutchinson and S. Montserrat, Thermochim. Acta, 286 (1996) 263.
26 B. Wunderlich, A. Boller, I. Okazaki and S. Kreitmeier, J. Thermal Anal., 47 (1996) 1013.
27 B. Wunderlich and I. Okazaki, Polym. Mater. Sci. Eng., 76 (1997) 217.
28 D. J. Hourston, M. Song, A. Hammiche, H. M. Pollock and M. Reading, Polymer, 37 (1996) 243.
29 Y. P. Khanna, W. P. Kuhn and W. J. William, Macromolecules, 28 (1995) 2644.
30 G. van Assche, A. van Hemelrijck, H. Rahier and B. van Mele, Thermochim. Acta, 268 (1995) 121.
31 G. van Assche, A. van Hemelrijck, H. Rahier and B. van Mele, Thermochim. Acta, 286 (1996) 209.
32 M.-J. Shim and S.-W. Kim, Mater. Chem. Phys., 47 (1997) 198.
33 G. Maistros, Q. P. V. Fontana, D. Attwood and J. S. Hudd, J. Mater. Sci. Lett., 16 (1997) 273.
34 M. Song, A. Hammiche, H. M. Pollock, D. J. Hourston and M. Reading, Polymer, 37 (1996) 5661.
35 G. O. R. van Ekenstein, G. ten Brinke and T. S. Ellis, Polym. Mater. Sci. Eng., 76 (1997) 219.
36 S. R. Sauerbrunn and L. Thomas, Am. Lab., 27 (1995) 19.
37 Y. Jin, J. Bonilaa, Y.-G. Lin, J. Morgan, L. McCracken and J. Carnahan, J. Thermal Anal., 46 (1996) 1047.
38 I. Okazaki and B. Wunderlich, Macromol. Rapid Commun., 18 (1997) 313.
39 I. Okazaki and B. Wunderlich, Macromolecules, 30 (1997) 1758.
40 A. Toda, T. Oda, S. Masamichi and Y. Saruyama, Polymer, 38 (1997) 231.
41 V. B. F. Mathot, Calorimetry and Thermal Analysis of Polymers, Hanser Publishers 1994, 105.
42 T. Ozawa and K. Kanari, Thermochim. Acta, 253 (1995) 183.
43 E. Donth, Glasubergang, Akademieverlag, Berlin 1981.
44 E. Donth, J. Non. Cryst. Solids, 53 (1982) 325.
45 E. J. Donth, Relaxation and Thermodynamics of Polymers; Glass transition, Akademie Verlag GmbH 1992.
46 V. A. Bershstein and V. M. Egorov, Differential Scanning Calorimetry of Polymers, Ellis Horwood 1994.
47 P. H. Lindemeyer, J. Polym. Sci. Polym. Phys. Ed., 17 (1979) 1965.